

Causal Architecture in Hidden Quantum Markov Models

February 24, 2026

Abdessatar Souissi

Department of Management Information Systems, College of Business and Economics,
Qassim University, Buraydah 51452, Saudi Arabia
a.souaissi@qu.edu.sa

Abdessatar Barhoumi

Department of Mathematics and Statistics, College of Science,
King Faisal University, Al-Ahsa P.O.Box: 400, 31982, Saudi Arabia
abarhoumi@kfu.edu.sa

Abstract

We introduce a class of causal hidden quantum Markov models (cHQMMs) that refine standard HQMMs by explicitly reversing the order between hidden updates and emissions. Through a minimal qubit model, we show that the conventional “emission–then–transition” and the alternative “transition–then–emission” architectures generally generate nonequivalent quantum processes, with distinct temporal correlation structures and different patterns of entanglement across time. At the same time, we prove that these two classes coincide for entangled lifting of classical hidden Markov models, where they share the same classical reduced process, thereby identifying a sharp boundary between classical and genuinely quantum hidden memory. These features suggest potential utility for modeling and analyzing quantum memory in sequential quantum processes.

1 Introduction

Many time-dependent phenomena are best thought of as being driven by an underlying “memory” that keeps track of what happened before and feeds this information forward in time. Hidden Markov models (HMMs) [31, 27] make this idea precise: a latent chain $(X_n)_{n \in \mathbb{N}}$ plays the role of the memory, and a sequence of observations $(Y_n)_{n \in \mathbb{N}}$ records what we actually measure at each step. At every time m , the update from X_{m-1} to (X_m, Y_m) factorises as

$$\mathbb{P}(x_m, y_m \mid x_{m-1}) = \underbrace{\mathbb{P}(x_m \mid x_{m-1})}_{\text{transition}} \underbrace{\mathbb{P}(y_m \mid x_m)}_{\text{emission}}, \quad Y_m \perp\!\!\!\perp X_{m+1} \mid X_m,$$

so the hidden chain is exactly the finite-memory mechanism that generates all temporal correlations in the data. Because the transition and emission terms are ordinary conditional probabilities, it makes no practical difference whether we write “transition then emission” or “emission then transition”: the causal content is entirely in these scalar laws, and this commutativity is what keeps classical HMMs both conceptually simple and computationally efficient [40, 39].

In the quantum setting, the picture becomes substantially more delicate: quantum operations are intrinsically non-commutative, and causal structure has to be formulated directly in terms of completely positive maps, rather than scalar conditional probabilities [41, 42]. Several extensions of hidden quantum Markov models (HQMMs) have been developed in this spirit, ranging from many-body and tensor-network descriptions of quantum states to quantum machine-learning models for sequential data and quantum information tasks [26, 37, 10]. A fully quantum–probabilistic framework for HQMMs was established in [1], in which the hidden dynamics is a quantum Markov chain in the sense of [4, 5] and the diagonal restriction of the resulting process reproduces a genuine classical HMM. This hybrid structure—quantum memory with a classical “shadow”—is particularly attractive for near-term implementations, where hybrid quantum–classical architectures and NISQ devices are already being used to simulate noisy channels and to design robust algorithms under realistic noise and resource constraints [11, 12, 8].

Concretely, the hidden system is described by local matrix algebras $\mathcal{B}_{H;n} \cong \mathcal{B}(\mathcal{H})$ (with $\dim \mathcal{H} = N$ and a preferred orthonormal basis $\{|i\rangle\}_{1 \leq i \leq N}$), assembled into an infinite tensor product $\bigotimes_{n \in \mathbb{N}} \mathcal{B}_{H;n}$, and evolves via a family of transition expectations

$$\mathcal{E}_{H;n} : \mathcal{B}_{H;n} \otimes \mathcal{B}_{H;n+1} \rightarrow \mathcal{B}_{H;n},$$

which are completely positive and unital, and thus admit dual quantum channels $\mathcal{E}_{H;n}^* : \mathfrak{S}(\mathcal{H}) \rightarrow \mathfrak{S}(\mathcal{H} \otimes \mathcal{H})$, where $\mathfrak{S}(\mathcal{H})$ denotes the set of density operators on \mathcal{H} , i.e. all positive semidefinite trace-one operators on \mathcal{H} . The observable system is encoded in local algebras $\mathcal{B}_{O;n} \cong \mathcal{B}(\mathcal{K})$ (with $\dim \mathcal{K} = M$ and basis $\{|e_j\rangle\}_{1 \leq j \leq M}$), forming $\bigotimes_{n \in \mathbb{N}} \mathcal{B}_{O;n}$, and couples to the hidden chain through emission expectations

$$\mathcal{E}_{H,O;n} : \mathcal{B}_{H;n} \otimes \mathcal{B}_{O;n} \rightarrow \mathcal{B}_{H;n},$$

which are again completely positive and unital, with dual channels $\mathcal{E}_{H,O;n}^* : \mathfrak{S}(\mathcal{H}) \rightarrow \mathfrak{S}(\mathcal{H} \otimes \mathcal{K})$.

The non-commutativity of the order in which we apply $\mathcal{E}_{H;n}$ and $\mathcal{E}_{H,O;n}$ means that the two causal prescriptions—“emission–then–transition” and “transition–then–emission”—are not just two ways of writing the same update, but two genuinely different ways of wiring the same local maps into a one-step HQMM. In [1] the emission–then–transition prescription was analysed in depth, leading to HQMMs with non-trivial entanglement structure [36] and to a flexible representation of important classes of matrix product states [34]; related constructions have been shown to capture, in particular, the entanglement and topological features of AKLT-type ground states [35].

In this paper we compare two causal architectures for HQMMs: emission–then–transition (conventional) and transition–then–emission (causal). We show that, even with the same local quantum maps $\mathcal{E}_{H;n}$ and $\mathcal{E}_{H,O;n}$, these two time orderings can generate genuinely different dynamics. For the conventional HQMM we take inputs $X_{H,O} \in \mathcal{B}_{H;n} \otimes \mathcal{B}_{O;n}$ and $X_{H;n+1} \in \mathcal{B}_{H;n+1}$, and define the emission–then–transition block map

$$\mathcal{F}^{(n)}(X_{H,O} \otimes X_{n+1}) = \mathcal{E}_{H;n}(\mathcal{E}_{H,O;n}(X_{H,O}) \otimes X_{H;n+1}),$$

while for the causal HQMM we take $X_{H;n,n+1} \in \mathcal{B}_{H;n} \otimes \mathcal{B}_{H;n+1}$ and $X_O \in \mathcal{B}_{O;n}$, and define the transition–then–emission map

$$\mathcal{G}^{(n)}(X_{H;n,n+1} \otimes X_O) = \mathcal{E}_{H,O;n}(\mathcal{E}_{H;n}(X_{H;n,n+1}) \otimes X_O).$$

The adjective “causal” is used here in a minimal, operator sense: in $\mathcal{G}^{(n)}$ the observation at time n depends on the hidden degrees of freedom only through the updated channel $\mathcal{E}_{H;n}$, so the output is caused by the post-update hidden configuration, whereas in $\mathcal{F}^{(n)}$ it is caused by the pre-update one. In a classical HMM, where conditional probabilities commute, this ordering is invisible; in the

quantum case the non-commutativity of $\mathcal{E}_{H;n}$ and $\mathcal{E}_{H,O;n}$ makes the two wirings genuinely different and, in principle, operationally distinguishable.

To compare the two architectures more concretely, we fix effects in the Heisenberg picture and look at the corresponding dual maps in the Schrödinger picture. Let $\text{Eff}(\mathcal{H})$ denote the effect algebra $\{a \in \mathcal{B}(\mathcal{H}) \mid 0 \leq a \leq \mathbb{I}\}$ on the hidden Hilbert space and $\text{Eff}(\mathcal{K})$ the set of effect on the output space [24, 22]. For fixed effects $a \in \text{Eff}(\mathcal{H})$ and $b \in \text{Eff}(\mathcal{K})$, inserting a and b in the appropriate legs and then dualising defines one-step hidden channels $\mathcal{F}_{a,b}^{(n)*}$ and $\mathcal{G}_{a,b}^{(n)*}$ acting on hidden states: informally, $\mathcal{F}_{a,b}^{(n)*}$ is the Schrödinger dual of the map $X \mapsto \mathcal{F}^{(n)}((a \otimes b) \otimes X)$, and $\mathcal{G}_{a,b}^{(n)*}$ is the dual of $X \mapsto \mathcal{G}^{(n)}((a \otimes X) \otimes b)$. We then show, via a minimal qubit model (hidden and output both two-dimensional) [17, 18, 43], that these two induced channels $\mathcal{F}_{a,b}^{(n)*}$ and $\mathcal{G}_{a,b}^{(n)*}$ are different for generic choices of hidden unitaries and non-trivial effects $a \in \text{Eff}(\mathcal{H})$, $b \in \text{Eff}(\mathcal{K})$: their Choi–Jamiołkowski operators [19, 20] are not equal, their diamond distance is strictly positive, and their entanglement spectra disagree, so the conventional and causal HQMMs have genuinely different entanglement structures and give rise to distinct optimal discrimination strategies.

A particularly clear situation where the two causal stories agree at the classical level is provided by entangled hidden Markov models [36]. Starting from a classical HMM $\lambda = (\boldsymbol{\pi}, \boldsymbol{\Pi}, \mathbf{Q})$ with hidden state set I_H , output set I_O , transition matrices $\Pi_n = (\Pi_{n,ij})$ and emission kernels $Q_j^{(n)}(k)$, we realize the hidden system on \mathcal{H} with basis $\{|i\rangle\}_{i \in I_H}$ and outputs on \mathcal{K} with basis $\{|e_k\rangle\}_{k \in I_O}$. The transitions of the hidden entangled Markov chains [2, 3] are encoded by a partial isometry $V_{H;n} : \mathcal{H} \rightarrow \mathcal{H} \otimes \mathcal{H}$, $V_{H;n}|i\rangle = \sum_{j \in I_H} \sqrt{\Pi_{n,ij}} |i, j\rangle$, inducing $\mathcal{E}_{H;n}(X) = V_{H;n}^* X V_{H;n}$; the emissions are encoded by $V_{H,O;n} : \mathcal{H} \rightarrow \mathcal{H} \otimes \mathcal{K}$, $V_{H,O;n}|j\rangle = \sum_{k \in I_O} \sqrt{Q_j^{(n)}(k)} |j, e_k\rangle$, inducing $\mathcal{E}_{H,O;n}(Y) = V_{H,O;n}^* Y V_{H,O;n}$. These expectations preserve the diagonal matrix units in the preferred bases and reproduce exactly the classical transition and emission probabilities on diagonals. In this entangled HMM setting, one checks on diagonal tensors such as $|i\rangle\langle i| \otimes |e_k\rangle\langle e_k|$ and their time-shifted versions that $\mathcal{F}^{(n)}$ and $\mathcal{G}^{(n)}$ act identically on all diagonal observables, so the associated conventional and causal HQMMs induce the same classical law on the diagonal subalgebra, even though they still define distinct quantum processes on off-diagonal operators.

From a quantum-memory perspective, the way we wire the hidden and emission maps determines how information is stored, propagated, and accessed over time. In topological quantum memories, for example, information is encoded in protected global degrees of freedom and becomes accessible only through carefully structured operations, highlighting how storage and readout are constrained by the underlying dynamics [13, 16]. Recent work on hidden quantum memory makes a similar point in a different setting: even when the observed statistics appear Markovian, the generating process can still rely on genuinely quantum memory resources that are only revealed by suitable probes [38, 14].

Viewed in this light, our two causal architectures are not just alternative parameterisations of a model, but two distinct ways of embedding and interrogating finite quantum memory. They provide explicit, operator-level mechanisms for deciding when and how past information is written into the hidden system and when it can be read out through the observations, and thus tie directly into broader efforts to design efficient, robust memory in quantum processes and adaptive agents [15, 33, 45].

The paper is organised as follows. Section 2 reviews basic tools from operator algebras and quantum information. Section 3 introduces causal HQMMs and discuss the two causal architectures. Section 4 presents a minimal qubit HQMM separating these architectures at the channel level. Section 5 studies entangled HMMs and identifies a regime where the architectures agree. Section 6 discusses implications and future directions.

2 Preliminaries

Let \mathcal{A} and \mathcal{B} be finite-dimensional C^* -algebras. A linear map $\mathcal{E} : \mathcal{A} \rightarrow \mathcal{B}$ is called positive if $\mathcal{E}(X) \geq 0$ whenever $X \geq 0$. It is called *completely positive* (CP) if, for every $n \in \mathbb{N}$, its matrix amplification $\mathcal{E}^{(n)} : M_n(\mathcal{A}) \rightarrow M_n(\mathcal{B})$, defined by $\mathcal{E}^{(n)}([X_{ij}]) = [\mathcal{E}(X_{ij})]$, is positive. A linear map $\mathcal{E} : \mathcal{A} \otimes \mathcal{B} \rightarrow \mathcal{A}$ is called a *transition expectation* if it is completely positive and normalised, in the sense that $\mathcal{E}(\mathbb{I}_{\mathcal{A}} \otimes \mathbb{I}_{\mathcal{B}}) = \mathbb{I}_{\mathcal{A}}$. This notion, introduced in the operator-algebraic formulation of QMCs [4, 5]. One may regard \mathcal{E} as a non-commutative analogue of a conditional expectation with respect to the second tensor component: it “integrates out” the algebra \mathcal{B} while preserving the unit and the order structure of \mathcal{A} .

Throughout, all Hilbert spaces are complex and finite-dimensional. For a Hilbert space \mathcal{H} , we denote by $\mathcal{B}(\mathcal{H})$ the C^* -algebra of all bounded linear operators on \mathcal{H} . In the concrete case $\mathcal{A} = \mathcal{B}(\mathcal{H})$ and $\mathcal{B} = \mathcal{B}(\mathcal{K})$, a transition expectation $\mathcal{E} : \mathcal{B}(\mathcal{H}) \otimes \mathcal{B}(\mathcal{K}) \rightarrow \mathcal{B}(\mathcal{H})$ can be written, in finite dimensions, in Kraus form as

$$\mathcal{E}(X) = \sum_{i=1}^r V_i^* X V_i, \quad \forall X \in \mathcal{B}(\mathcal{H} \otimes \mathcal{K})$$

where the Kraus operators $V_i : \mathcal{H} \rightarrow \mathcal{H} \otimes \mathcal{K}$ satisfy $\sum_i V_i^* V_i = \mathbb{I}_{\mathcal{H}}$, where the Kraus operators $V_i : \mathcal{K} \rightarrow \mathcal{H}$ satisfy $\sum_i V_i^* V_i = \mathbb{I}_{\mathcal{H}}$. We distinguish density operators, subnormalised states, and effects using the Löwner order on self-adjoint operators. For $A, B \in \mathcal{B}(\mathcal{H})_{\text{sa}}$ we write

$$A \preceq B \quad \text{iff} \quad B - A \succeq 0,$$

that is, $B - A$ is positive semidefinite.

The set of (normalised) density operators on \mathcal{H} is

$$\mathfrak{S}(\mathcal{H}) := \{\rho \in \mathcal{B}(\mathcal{H}) \mid \rho \succeq 0, \text{Tr}(\rho) = 1\},$$

and represents the quantum states of \mathcal{H} . The *effect set* on \mathcal{H} is defined by

$$\text{Eff}(\mathcal{H}) := \{e \in \mathcal{B}(\mathcal{H}) \mid 0 \preceq e \preceq \mathbb{I}_{\mathcal{H}}\},$$

and its elements represent quantum events, i.e. yes–no measurements with outcome probabilities $\text{Tr}(\rho e)$ for $\rho \in \mathfrak{S}(\mathcal{H})$. The Hilbert–Schmidt inner product $\langle \rho, X \rangle = \text{Tr}(\rho X)$ on $\mathfrak{S}(\mathcal{H}) \times \mathcal{B}(\mathcal{H})$ induces a unique adjoint map $\mathcal{E}_* : \mathfrak{S}(\mathcal{H}) \rightarrow \mathfrak{S}(\mathcal{H} \otimes \mathcal{K})$ defined by the single duality relation

$$\text{Tr}(\mathcal{E}_*(\rho)X) = \text{Tr}(\rho \mathcal{E}(X)) \tag{1}$$

for all $\rho \in \mathfrak{S}(\mathcal{H})$ and all $X \in \mathcal{B}(\mathcal{H} \otimes \mathcal{K})$. In Kraus form this adjoint is $\mathcal{E}_*(\rho) = \sum_i V_i \rho V_i^*$, which is a completely positive, trace-preserving map on states.

At the level of quantum information, a channel $\Phi : \mathfrak{S}(\mathcal{H}) \rightarrow \mathfrak{S}(\mathcal{H}')$ represents a causal influence from the input system \mathcal{H} to the output system $\mathfrak{S}(\mathcal{H}')$: interventions on the input density matrix can change the statistics of all future measurements on the enlarged system, but not conversely. The dual map \mathcal{E} propagates observables backwards along this causal arrow, implementing the Heisenberg-picture dynamics of a quantum Markov chain.

We now specialise to the setting of hidden quantum Markov models. Let \mathcal{H} be an N -dimensional Hilbert space representing the hidden, or internal, degrees of freedom. We fix an orthonormal basis $\{|j\rangle : j \in I_H\}$ with $I_H = \{1, \dots, N\}$, and denote the associated hidden observable algebra by $\mathcal{B}_H := \mathcal{B}(\mathcal{H})$. Similarly, let \mathcal{K} be an M -dimensional Hilbert space modelling the output or

observation space, with orthonormal basis $\{|e_k\rangle : k \in I_O\}$, $I_O = \{1, \dots, M\}$, and observable algebra $\mathcal{B}_O := \mathcal{B}(\mathcal{K})$. Heuristically, \mathcal{B}_H contains the “latent quantum causes” and \mathcal{B}_O contains the “observable effects” in the sense of quantum cause–effect identification.

Time is discrete and indexed by $\mathbb{N} = \{0, 1, 2, \dots\}$. At each time $n \in \mathbb{N}$, we attach Hilbert spaces $\mathcal{H}_n \simeq \mathcal{H}$ and $\mathcal{K}_n \simeq \mathcal{K}$ with observable algebras

$$\mathcal{B}_{H;n} := \mathcal{B}(\mathcal{H}_n) \simeq \mathcal{B}_H, \quad \mathcal{B}_{O;n} := \mathcal{B}(\mathcal{K}_n) \simeq \mathcal{B}_O.$$

The local hidden–output algebra at time n is the spatial tensor product $\mathcal{B}_{H,O;n} := \mathcal{B}_{H;n} \otimes \mathcal{B}_{O;n}$, which encodes all observables acting jointly on the hidden subsystem and its associated output at that instant. For a finite time interval $[0, n] = \{0, 1, \dots, n\}$, we consider the tensor product algebras

$$\mathcal{B}_{H;[0,n]} := \bigotimes_{m=0}^n \mathcal{B}_{H;m}, \quad \mathcal{B}_{O;[0,n]} := \bigotimes_{m=0}^n \mathcal{B}_{O;m}, \quad \mathcal{B}_{H,O;[0,n]} := \bigotimes_{m=0}^n \mathcal{B}_{H,O;m},$$

describing, respectively, the hidden history, the observable history, and the full hidden–observable history over $[0, n]$. The corresponding local (finitely supported) algebras are the algebraic inductive limits

$$\mathcal{B}_{H;\text{loc}} := \bigcup_{n \geq 0} \mathcal{B}_{H;[0,n]}, \quad \mathcal{B}_{O;\text{loc}} := \bigcup_{n \geq 0} \mathcal{B}_{O;[0,n]}, \quad \mathcal{B}_{H,O;\text{loc}} := \bigcup_{n \geq 0} \mathcal{B}_{H,O;[0,n]}.$$

Their norm closures in the operator norm yield the quasi-local C^* -algebras

$$\mathcal{B}_{H;\mathbb{N}} := \bigotimes_{n \in \mathbb{N}} \mathcal{B}_{H;n}, \quad \mathcal{B}_{O;\mathbb{N}} := \bigotimes_{n \in \mathbb{N}} \mathcal{B}_{O;n}, \quad \mathcal{B}_{H,O;\mathbb{N}} := \bigotimes_{n \in \mathbb{N}} \mathcal{B}_{H,O;n}.$$

The reader is referred to [9] for a detailed presentation of quasi-local algebras. Within this framework, a hidden quantum Markov model is specified by an initial hidden state $\phi_{H,0} : \mathcal{B}_H \rightarrow \mathbb{C}$ and two families of transition expectations that describe, respectively, the internal propagation of the hidden chain and its causal influence on the output. The hidden dynamics is given by CPIP maps $\mathcal{E}_{H;n} : \mathcal{B}_{H;n} \otimes \mathcal{B}_{H;n+1} \rightarrow \mathcal{B}_{H;n}$ for $n \geq 0$. Via Hilbert–Schmidt duality, each $\mathcal{E}_{H;n}$ induces a channel $(\mathcal{E}_{H;n})_* : \mathfrak{S}(\mathcal{H}_n) \rightarrow \mathfrak{S}(\mathcal{H}_n \otimes \mathcal{H}_{n+1})$ defined by $\text{Tr}((\mathcal{E}_{H;n})_*(\rho_{H;n})X) = \text{Tr}(\rho_{H;n} \mathcal{E}_{H;n}(X))$ for all $\rho_{H;n} \in \mathfrak{S}(\mathcal{H}_n)$, $X \in \mathcal{B}(\mathcal{H}_n \otimes \mathcal{H}_{n+1})$.

In this subsection we recast the comparison between the conventional and causal architectures at a fixed time-step in the language of quantum channel discrimination. We begin with a rigorous definition of the diamond distance between two completely positive trace-preserving (CPTP) maps and then specialize to the dual one-step hidden channels induced by the block maps of the two architectures. This allows us to quantify, in a fully operational way, how distinguishable the two temporal orders are, in the sense of optimal one-shot channel discrimination [30].

Definition 2.1 (Diamond distance). *Let \mathcal{H}_{in} and \mathcal{H}_{out} be finite-dimensional Hilbert spaces and let*

$$\Phi_1, \Phi_2 : \mathcal{B}(\mathcal{H}_{\text{in}}) \rightarrow \mathcal{B}(\mathcal{H}_{\text{out}})$$

be quantum channels (normal, completely positive and trace-preserving). The diamond distance between Φ_1 and Φ_2 is defined by

$$\|\Phi_1 - \Phi_2\|_{\diamond} := \sup_{d \in \mathbb{N}} \sup_{\rho \in \mathfrak{S}(\mathcal{H}_{\text{in}} \otimes \mathbb{C}^d)} \|(\Phi_1 \otimes \text{id}_d)(\rho) - (\Phi_2 \otimes \text{id}_d)(\rho)\|_1$$

where $\|\cdot\|_1$ denotes the trace norm and id_d is the identity channel on $\mathcal{B}(\mathbb{C}^d)$. For finite-dimensional \mathcal{H}_{in} the supremum may be restricted to $d = \dim \mathcal{H}_{\text{in}}$.

The diamond distance is the canonical measure of single-use distinguishability of quantum channels. If one is given a single use of an unknown channel, promised to be either Φ_1 or Φ_2 with equal a priori probabilities, then the optimal success probability $p_{\text{succ}}^{(1)}$ in identifying the channel satisfies

$$p_{\text{succ}}^{(1)} = \frac{1}{2} + \frac{1}{4} \|\Phi_1 - \Phi_2\|_{\diamond},$$

so that $\|\Phi_1 - \Phi_2\|_{\diamond} = 0$ if and only if Φ_1 and Φ_2 are operationally indistinguishable in one use.

We next introduce the Choi–Jamiołkowski representation of a channel and recall its relation to the diamond norm. Fix an orthonormal basis $\{|i\rangle\}_{i=1}^{d_{\text{in}}}$ of \mathcal{H}_{in} and consider the (unnormalised) maximally entangled vector

$$|\Omega\rangle := \sum_{i=1}^{d_{\text{in}}} |i\rangle \otimes |i\rangle \in \mathcal{H}_{\text{in}} \otimes \mathcal{H}_{\text{in}}.$$

Definition 2.2 (Choi operator). *For a linear map $\Phi : \mathcal{B}(\mathcal{H}_{\text{in}}) \rightarrow \mathcal{B}(\mathcal{H}_{\text{out}})$, its Choi operator is*

$$J(\Phi) := (\text{id} \otimes \Phi)(|\Omega\rangle\langle\Omega|) \in \mathcal{B}(\mathcal{H}_{\text{in}} \otimes \mathcal{H}_{\text{out}}).$$

If Φ is CPTP, then $J(\Phi) \geq 0$ and $\text{Tr}_{\text{out}} J(\Phi) = \mathbb{I}_{\mathcal{H}_{\text{in}}}$.

The assignment $\Phi \mapsto J(\Phi)$ is injective and affine, and there are well-known bounds relating the diamond norm of $\Phi_1 - \Phi_2$ to the trace norm of the Choi difference $J(\Phi_1) - J(\Phi_2)$. In particular, one has

$$\frac{1}{d_{\text{in}}} \|J(\Phi_1) - J(\Phi_2)\|_1 \leq \|\Phi_1 - \Phi_2\|_{\diamond} \leq \|J(\Phi_1) - J(\Phi_2)\|_1 \quad (2)$$

where $d_{\text{in}} = \dim \mathcal{H}_{\text{in}}$. The lower bound may be viewed as a consequence of evaluating the supremum in the diamond norm on suitably chosen input states that are close to maximally entangled, while the upper bound follows from an operator-space duality argument.

3 Causal hidden quantum Markov models

The coupling between hidden and observable degrees of freedom is encoded by emission expectations $\mathcal{E}_{H,O;n} : \mathcal{B}_{H;n} \otimes \mathcal{B}_{O;n} \rightarrow \mathcal{B}_{H;n}$. For $b_n \in \mathcal{B}_{O;n}$, the dual map $(\mathcal{E}_{H,O;n})_* : \mathfrak{S}(\mathcal{H}_n) \rightarrow \mathfrak{S}(\mathcal{H}_n \otimes \mathcal{K}_n)$ is the quantum operation that produces an output system \mathcal{K}_n conditioned on the hidden state at time n , and formalises the causal arrow $H_n \rightarrow O_n$. Tracing out the hidden algebra yields an induced process on $\mathcal{B}_{O;\mathbb{N}}$ whose temporal correlations may violate classical Markov conditions and appear “non-Markovian”; in the process-tensor viewpoint [25] this non-Markovianity can be understood as the imprint of genuine quantum memory living in $\mathcal{B}_{H;\mathbb{N}}$ and propagating via the $\mathcal{E}_{H;n}$.

Given local elements $a_n \in \mathcal{B}_{H;n}$, $a_{n+1} \in \mathcal{B}_{H;n+1}$, and $b_n \in \mathcal{B}_{O;n}$, the one-step map

$$\mathcal{F}_{a_n, b_n}^{(n)}(a_{n+1}) := \mathcal{E}_{H;n}(\mathcal{E}_{H,O;n}(a_n \otimes b_n) \otimes a_{n+1}), \quad (3)$$

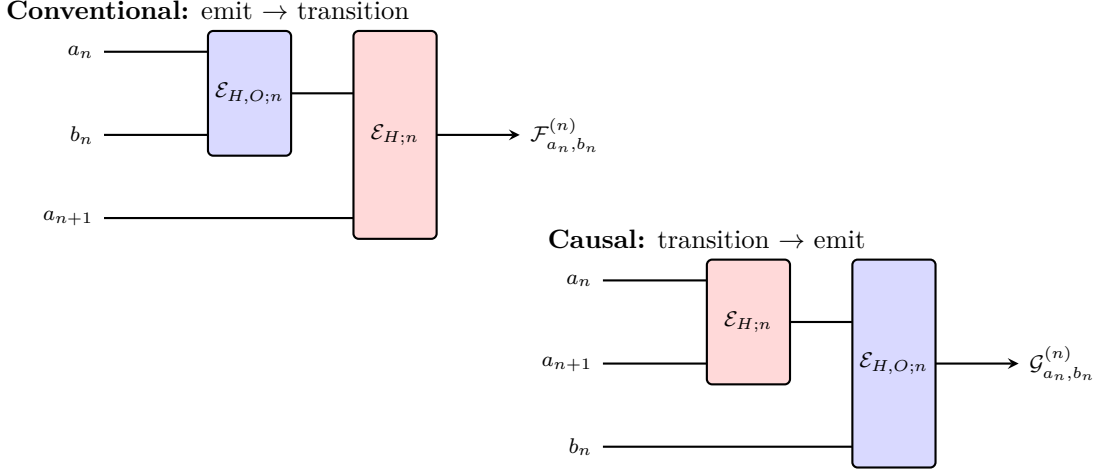
realises the conventional HQMM causal order: the hidden system at time n first influences the output at time n through $\mathcal{E}_{H,O;n}$, then is propagated internally to time $n+1$ via $\mathcal{E}_{H;n}$. The alternative one-step map

$$\mathcal{G}_{a_n, b_n}^{(n)}(a_{n+1}) := \mathcal{E}_{H,O;n}(\mathcal{E}_{H;n}(a_n \otimes a_{n+1}) \otimes b_n), \quad (4)$$

built from a second family $\tilde{\mathcal{E}}_{H,O;n}$, swaps this order: the hidden chain first advances from H_n to H_{n+1} and only the updated hidden configuration acts as the cause for the observation at time

n . In both cases, composing the maps $\mathcal{F}_{a_n, b_n}^{(n)}$ or $\mathcal{G}_{a_n, b_n}^{(n)}$ and evaluating with $\phi_{H,0}$ produces a state on $\mathcal{B}_{H,O;\mathbb{N}}$, and the restriction to $\mathcal{B}_{O;\mathbb{N}}$ is an output process whose temporal structure reflects the chosen causal order.

The next pair of diagrams summarises these two one-step updates in a way that makes this causal structure manifest. For clarity and symmetry, the conventional diagram is placed in the upper-left, while the causal diagram is placed in the lower-right; the red and blue blocks are chosen so that the "role" of each block is exchanged between the two diagrams.



Although the two architectures are built from the same families of completely positive maps, they implement distinct causal relationships between hidden and observable subsystems. In particular, since $\mathcal{E}_{H;n}$ and $\mathcal{E}_{H,O;n}$ do not commute in general, the one-step maps $\mathcal{F}_{a_n, b_n}^{(n)}$ and $\mathcal{G}_{a_n, b_n}^{(n)}$ give rise to non-equivalent hidden quantum Markov processes.

Definition 3.1. [1][Conventional hidden quantum Markov model] A conventional hidden quantum Markov model (conventional HQMM) is a quadruple

$$\Xi_{\text{conv}} = (\phi_{H,0}, (\mathcal{E}_{H;n})_{n \geq 0}, (\mathcal{E}_{H,O;n})_{n \geq 0}, (\mathcal{F}^{(n)})_{n \geq 0}),$$

where:

- $\phi_{H,0} : \mathcal{B}_H \rightarrow \mathbb{C}$ is an initial state on the hidden algebra;
- $\mathcal{E}_{H;n} : \mathcal{B}_{H;n} \otimes \mathcal{B}_{H;n+1} \rightarrow \mathcal{B}_{H;n}$ are hidden transition expectations;
- $\mathcal{E}_{H,O;n} : \mathcal{B}_{H;n} \otimes \mathcal{B}_{O;n} \rightarrow \mathcal{B}_{H;n}$ are emission expectations;
- for each time n , the one-step block map

$$\mathcal{F}^{(n)} : \mathcal{B}_{H;n} \otimes \mathcal{B}_{O;n} \otimes \mathcal{B}_{H;n+1} \rightarrow \mathcal{B}_{H;n}$$

is defined, for local inputs $a_n \in \mathcal{B}_{H;n}$, $b_n \in \mathcal{B}_{O;n}$, $X \in \mathcal{B}_{H;n+1}$, by

$$\mathcal{F}_{a_n, b_n}^{(n)}(X) := \mathcal{E}_{H;n}(\mathcal{E}_{H,O;n}(a_n \otimes b_n) \otimes X).$$

For a local tensor observable $\bigotimes_{m=0}^n (a_m \otimes b_m) \in \mathcal{B}_{H,O;[0,n]}$, the finite-time joint expectation of the conventional HQMM is given by

$$\varphi_{H,O} \left(\bigotimes_{m=0}^n (a_m \otimes b_m) \right) := \phi_{H,0} \circ \mathcal{F}_{a_0, b_0}^{(0)} \circ \mathcal{F}_{a_1, b_1}^{(1)} \circ \dots \circ \mathcal{F}_{a_n, b_n}^{(n)}(\mathbb{I}_{H;n+1}) \quad (5)$$

These linear functionals are compatible for different n and extend uniquely (by the usual projective-limit construction) to a state $\varphi_{H,O}$ on the quasi-local algebra $\mathcal{B}_{H,O;\mathbb{N}}$. The corresponding hidden and observable marginals are defined by restriction:

$$\varphi_H := \varphi_{H,O} \upharpoonright_{\mathcal{B}_{H;\mathbb{N}}}, \quad \varphi_O := \varphi_{H,O} \upharpoonright_{\mathcal{B}_{O;\mathbb{N}}}$$

Definition 3.2 (Causal hidden quantum Markov model). A causal hidden quantum Markov model (causal HQMM) is a quadruple

$$\Xi_{\text{caus}} = (\phi_{H,0}, (\mathcal{E}_{H;n})_{n \geq 0}, (\mathcal{E}_{H,O;n})_{n \geq 0}, (\mathcal{G}^{(n)})_{n \geq 0}),$$

with the same initial hidden state $\phi_{H,0}$ and the same families of hidden transition and emission expectations $(\mathcal{E}_{H;n})_{n \geq 0}$, $(\mathcal{E}_{H,O;n})_{n \geq 0}$ as above, but a different one-step composition rule encoded in the block maps $\mathcal{G}^{(n)}$. For each n , the block map

$$\mathcal{G}^{(n)} : \mathcal{B}_{H;n} \otimes \mathcal{B}_{O;n} \otimes \mathcal{B}_{H;n+1} \rightarrow \mathcal{B}_{H;n}$$

is defined, for $a_n \in \mathcal{B}_{H;n}$, $b_n \in \mathcal{B}_{O;n}$, $X \in \mathcal{B}_{H;n+1}$, by

$$\mathcal{G}_{a_n, b_n}^{(n)}(X) := \mathcal{E}_{H,O;n}(\mathcal{E}_{H;n}(a_n \otimes X) \otimes b_n).$$

For a local tensor $\bigotimes_{m=0}^n (a_m \otimes b_m) \in \mathcal{B}_{H,O;[0,n]}$, the finite-time joint expectation of the causal HQMM is then

$$\psi_{H,O} \left(\bigotimes_{m=0}^n (a_m \otimes b_m) \right) := \phi_{H,0} \circ \mathcal{G}_{a_0, b_0}^{(0)} \circ \mathcal{G}_{a_1, b_1}^{(1)} \circ \cdots \circ \mathcal{G}_{a_n, b_n}^{(n)}(\mathbb{I}_{H;n+1}), \quad (6)$$

which again extends uniquely to a state $\psi_{H,O}$ on $\mathcal{B}_{H,O;\mathbb{N}}$. The associated hidden and observable marginals are

$$\psi_H := \psi_{H,O} \upharpoonright_{\mathcal{B}_{H;\mathbb{N}}}, \quad \psi_O := \psi_{H,O} \upharpoonright_{\mathcal{B}_{O;\mathbb{N}}}.$$

From the perspective of quantum causal models, the ‘‘conventional’’ and ‘‘causal’’ HQMM architectures correspond to two inequivalent ways of realising the same underlying static causal graph at the level of channels: in the conventional case the edge $H_n \rightarrow O_n$ is implemented before $H_n \rightarrow H_{n+1}$, whereas in the causal case $H_n \rightarrow H_{n+1}$ is implemented first. Since $\mathcal{E}_{H;n}$ and $\mathcal{E}_{H,O;n}$ need not commute, the two resulting processes are generally different. Yet in both architectures, apparent non-Markovianity in the output algebra $\mathcal{B}_{O;\mathbb{N}}$ can be interpreted as the projection of a Markovian quantum causal dynamics on $\mathcal{B}_{H,O;\mathbb{N}}$ onto the observable sector, with the hidden algebra $\mathcal{B}_{H;\mathbb{N}}$ carrying the quantum memory that mediates the causal influence from past hidden configurations to future observations. This is the HQMM analogue of the no-retrocausality and faithfulness assumptions in quantum causal discovery [21].

In both cases, the triplet $(\phi_{H,0}, (\mathcal{E}_{H;n}), (\mathcal{E}_{H,O;n}))$ fixes the local building blocks (initial state, hidden transitions, and emission expectations), while the families $(\mathcal{F}^{(n)})_{n \geq 0}$ and $(\mathcal{G}^{(n)})_{n \geq 0}$ specify how these blocks are composed in time. It is precisely this choice of block maps—emission—then—transition in the conventional case, transition—then—emission in the causal case—that distinguishes the two HQMM architectures and leads to different joint states $\varphi_{H,O}$, $\psi_{H,O}$ and different marginals on the hidden and observable algebras.

Lemma 3.3. [Dual block maps in Kraus form] Fix a time step n and suppose that the hidden transition and emission expectations admit minimal Kraus decompositions

$$\mathcal{E}_{H;n}(X) = \sum_{\alpha=1}^{r_H} K_{H;\alpha}^* X K_{H;\alpha}, \quad \mathcal{E}_{H,O;n}(Y) = \sum_{\beta=1}^{r_O} K_{H,O;\beta}^* Y K_{H,O;\beta},$$

where $K_{H;\alpha} : \mathcal{H}_n \rightarrow \mathcal{H}_n \otimes \mathcal{H}_{n+1}$ and $K_{H,O;\beta} : \mathcal{H}_n \rightarrow \mathcal{H}_n \otimes \mathcal{K}_n$ satisfy $\sum_{\alpha} K_{H;\alpha}^* K_{H;\alpha} = \sum_{\beta} K_{H,O;\beta}^* K_{H,O;\beta} = \mathbb{I}_{\mathcal{H}_n}$. Let $\mathcal{F}_{a,b}^{(n)}$ and $\mathcal{G}_{a,b}^{(n)}$ be the block maps defined in (3) and (4), and let

$$\mathcal{F}_{a,b}^{(n)*}, \mathcal{G}_{a,b}^{(n)*} : \mathfrak{S}_{\leq 1}(\mathcal{H}_n) \rightarrow \mathfrak{S}(\mathcal{H}_{n+1})$$

denote their Schrödinger-picture duals with respect to the Hilbert–Schmidt pairing (1). Then, for every $\rho \in \mathfrak{S}(\mathcal{H}_n)$,

$$\begin{aligned} \mathcal{F}_{a,b}^{(n)*}(\rho) &= \sum_{\alpha=1}^{r_H} \text{Tr}_{\mathcal{H}_n} \left[K_{H;\alpha} \rho K_{H;\alpha}^* (\mathcal{E}_{H,O;n}(a \otimes b) \otimes \mathbb{I}_{\mathcal{H}_{n+1}}) \right] \\ &= \sum_{\alpha=1}^{r_H} \sum_{\beta=1}^{r_O} \text{Tr}_{\mathcal{H}_n} \left[K_{H;\alpha} \rho K_{H;\alpha}^* \left(K_{H,O;\beta}^* (a \otimes b) K_{H,O;\beta} \otimes \mathbb{I}_{\mathcal{H}_{n+1}} \right) \right] \end{aligned} \quad (7)$$

$$\begin{aligned} \mathcal{G}_{a,b}^{(n)*}(\rho) &= \sum_{\beta=1}^{r_O} \text{Tr}_{\mathcal{H}_n} \left[K_{H,O;\beta} \rho K_{H,O;\beta}^* (\mathcal{E}_{H;n}(a \otimes \mathbb{I}_{\mathcal{H}_{n+1}}) \otimes b) \right] \\ &= \sum_{\alpha=1}^{r_H} \sum_{\beta=1}^{r_O} \text{Tr}_{\mathcal{H}_n} \left[K_{H,O;\beta} \rho K_{H,O;\beta}^* \left(K_{H;\alpha}^* (a \otimes \mathbb{I}_{\mathcal{H}_{n+1}}) K_{H;\alpha} \otimes b \right) \right] \end{aligned} \quad (8)$$

where $\text{Tr}_{\mathcal{H}_n}$ denotes the partial trace over the hidden space at time n .

Proof. We prove the formula for $\mathcal{F}_{a,b}^{(n)*}$; the argument for $\mathcal{G}_{a,b}^{(n)*}$ is analogous. The duality relation (1) states that for all $\rho \in \mathfrak{S}(\mathcal{H}_n)$ and $X \in \mathcal{B}(\mathcal{H}_{n+1})$,

$$\text{Tr}(\mathcal{F}_{a,b}^{(n)*}(\rho) X) = \text{Tr}(\rho \mathcal{F}_{a,b}^{(n)}(X)).$$

Using (3) and the Kraus representation of $\mathcal{E}_{H;n}$, we obtain

$$\mathcal{F}_{a,b}^{(n)}(X) = \mathcal{E}_{H;n}(\mathcal{E}_{H,O;n}(a \otimes b) \otimes X) = \sum_{\alpha=1}^{r_H} K_{H;\alpha}^* (\mathcal{E}_{H,O;n}(a \otimes b) \otimes X) K_{H;\alpha}.$$

Hence

$$\text{Tr}(\rho \mathcal{F}_{a,b}^{(n)}(X)) = \sum_{\alpha=1}^{r_H} \text{Tr}(\rho K_{H;\alpha}^* (\mathcal{E}_{H,O;n}(a \otimes b) \otimes X) K_{H;\alpha}).$$

By cyclicity of the trace, each summand can be rewritten as

$$\text{Tr}\left(K_{H;\alpha} \rho K_{H;\alpha}^* (\mathcal{E}_{H,O;n}(a \otimes b) \otimes X)\right).$$

We now interpret this as a trace over $\mathcal{H}_n \otimes \mathcal{H}_{n+1}$ and factor it via the partial trace. For any operator M on $\mathcal{H}_n \otimes \mathcal{H}_{n+1}$ and X on \mathcal{H}_{n+1} , one has

$$\text{Tr}_{\mathcal{H}_n \otimes \mathcal{H}_{n+1}} [M(\mathbb{I}_{\mathcal{H}_n} \otimes X)] = \text{Tr}_{\mathcal{H}_{n+1}} [\text{Tr}_{\mathcal{H}_n}(M) X],$$

so with

$$M = K_{H;\alpha} \rho K_{H;\alpha}^* (\mathcal{E}_{H,O;n}(a \otimes b) \otimes \mathbb{I}_{\mathcal{H}_{n+1}})$$

we obtain

$$\text{Tr}\left(K_{H;\alpha} \rho K_{H;\alpha}^* (\mathcal{E}_{H,O;n}(a \otimes b) \otimes X)\right) = \text{Tr}_{\mathcal{H}_{n+1}} \left[\text{Tr}_{\mathcal{H}_n} \left(K_{H;\alpha} \rho K_{H;\alpha}^* (\mathcal{E}_{H,O;n}(a \otimes b) \otimes \mathbb{I}_{\mathcal{H}_{n+1}}) \right) X \right].$$

Summing over α and using linearity of the partial trace, we arrive at

$$\mathrm{Tr}(\rho \mathcal{F}_{a,b}^{(n)}(X)) = \mathrm{Tr}_{\mathcal{H}_{n+1}} \left(\left[\sum_{\alpha=1}^{r_H} \mathrm{Tr}_{\mathcal{H}_n} \left(K_{H;\alpha} \rho K_{H;\alpha}^* (\mathcal{E}_{H,O;n}(a \otimes b) \otimes \mathbb{I}_{\mathcal{H}_{n+1}}) \right) \right] X \right).$$

By the defining duality, the square bracket must coincide with $\mathcal{F}_{a,b}^{(n)*}(\rho)$, since this identity holds for all X . Thus

$$\mathcal{F}_{a,b}^{(n)*}(\rho) = \sum_{\alpha=1}^{r_H} \mathrm{Tr}_{\mathcal{H}_n} \left[K_{H;\alpha} \rho K_{H;\alpha}^* (\mathcal{E}_{H,O;n}(a \otimes b) \otimes \mathbb{I}_{\mathcal{H}_{n+1}}) \right].$$

Finally, inserting the Kraus expansion of $\mathcal{E}_{H,O;n}$,

$$\mathcal{E}_{H,O;n}(a \otimes b) = \sum_{\beta=1}^{r_O} K_{H,O;\beta}^* (a \otimes b) K_{H,O;\beta},$$

we obtain the first formula stated in the lemma.

The derivation for $\mathcal{G}_{a,b}^{(n)*}$ is identical in structure. Starting from (4), using the Kraus decomposition of $\mathcal{E}_{H,O;n}$, cycling the trace, and factorising via partial traces leads to

$$\mathrm{Tr}(\rho \mathcal{G}_{a,b}^{(n)}(X)) = \mathrm{Tr}_{\mathcal{H}_{n+1}} \left(\left[\sum_{\beta=1}^{r_O} \mathrm{Tr}_{\mathcal{H}_n} \left(K_{H,O;\beta} \rho K_{H,O;\beta}^* (\mathcal{E}_{H;n}(a \otimes \mathbb{I}_{\mathcal{H}_{n+1}}) \otimes b) \right) \right] X \right)$$

for all X . By uniqueness of the Hilbert–Schmidt dual, the bracketed operator is exactly $\mathcal{G}_{a,b}^{(n)*}(\rho)$, and expanding $\mathcal{E}_{H;n}$ in its Kraus form yields the second formula. This completes the proof. \square

4 A qubit HQMM: conventional vs. causal

In this section we exhibit a minimal qubit model [43] showing that the conventional and causal HQMM architectures are, in general, inequivalent as states on the underlying effect algebra. The construction is formulated in terms of the hidden and emission isometries $V_{H;n}$ and $V_{H,O;n}$ and the block maps $\mathcal{F}_{a,b}^{(n)}$ and $\mathcal{G}_{a,b}^{(n)}$ defined in (3) and (4).

We work at a fixed time step n and suppress the index n when no confusion can arise. The hidden spaces are $\mathcal{H}_n \simeq \mathbb{C}^2$ and $\mathcal{H}_{n+1} \simeq \mathbb{C}^2$ with computational bases $\{|0\rangle_n, |1\rangle_n\}$ and $\{|0\rangle_{n+1}, |1\rangle_{n+1}\}$, and the output space is $\mathcal{K}_n \simeq \mathbb{C}^2$ with basis $\{|e_0\rangle_n, |e_1\rangle_n\}$. We consider a hidden unitary rotation about the x -axis,

$$\sigma_x = \begin{pmatrix} 0 & 1 \\ 1 & 0 \end{pmatrix}, \quad U := \exp(-i\frac{\theta}{2}\sigma_x) = \cos(\frac{\theta}{2})\mathbb{I} - i\sin(\frac{\theta}{2})\sigma_x,$$

with parameter $0 < |\theta| < \pi$. The hidden Stinespring isometry is

$$V_{H;n} : \mathcal{H}_n \longrightarrow \mathcal{H}_n \otimes \mathcal{H}_{n+1}, \quad V_{H;n}|\psi\rangle_n := U|\psi\rangle_n \otimes |0\rangle_{n+1},$$

for all $|\psi\rangle_n \in \mathcal{H}_n$, so that $V_{H;n}^* V_{H;n} = \mathbb{I}_{\mathcal{H}_n}$. This induces the completely positive unital expectation

$$\mathcal{E}_{H;n}(X) := V_{H;n}^* X V_{H;n}, \quad X \in \mathcal{B}(\mathcal{H}_n \otimes \mathcal{H}_{n+1}),$$

and its dual Schrödinger channel

$$\mathcal{E}_{H;n*}(\rho) = V_{H;n} \rho V_{H;n}^*, \quad \rho \in \mathrm{Eff}(\mathcal{H}).$$

The emission step is a sharp measurement of the hidden qubit in the computational basis, with the outcome encoded into the output register. We choose the isometry

$$V_{H,O;n} : \mathcal{H}_n \longrightarrow \mathcal{H}_n \otimes \mathcal{K}_n, \quad V_{H,O;n}|0\rangle_n = |0\rangle_n \otimes |e_0\rangle_n, \quad V_{H,O;n}|1\rangle_n = |1\rangle_n \otimes |e_1\rangle_n,$$

so that $V_{H,O;n}^* V_{H,O;n} = \mathbb{I}_{\mathcal{H}_n}$. The corresponding emission expectation and its dual are

$$\mathcal{E}_{H,O;n}(Y) := V_{H,O;n}^* Y V_{H,O;n}, \quad \mathcal{E}_{H,O;n}^*(\rho) = V_{H,O;n} \rho V_{H,O;n}^*,$$

for $Y \in \mathcal{B}(\mathcal{H}_n \otimes \mathcal{K}_n)$ and $\rho \in \text{Eff}(\mathcal{H})$. Note that for $0 < |\theta| < \pi$ the hidden unitary U does not commute with the projectors $|0\rangle\langle 0|$ and $|1\rangle\langle 1|$, and hence the corresponding hidden and emission channels need not commute under composition.

4.1 Distinguishability of conventional and causal HQMMs

We fix the following effects at time n :

$$a := \mathbb{I}_{\mathcal{H}_n}, \quad b := |e_0\rangle_n \langle e_0| \in \text{Eff}(\mathcal{K}_n).$$

Then $a \otimes b = \mathbb{I}_{\mathcal{H}_n} \otimes |e_0\rangle_n \langle e_0|$ is an element of $\text{Eff}(\mathcal{H}_n \otimes \mathcal{K}_n)$ and satisfies

$$\mathcal{E}_{H,O;n}(a \otimes b) = \mathcal{E}_{H,O;n}(\mathbb{I} \otimes |e_0\rangle_n \langle e_0|) = |0\rangle_n \langle 0|.$$

We consider the one-step block maps $\mathcal{F}_{a,b}^{(n)}$ and $\mathcal{G}_{a,b}^{(n)}$ defined in (3) and (4), and their duals given in Lemma 3.3, specialised to this qubit setting.

Lemma 4.1. *In the qubit model above, for $(a, b) = (\mathbb{I}_{\mathcal{H}_n}, |e_0\rangle_n \langle e_0|)$ and any $0 < |\theta| < \pi$, the one-step dual maps $\mathcal{F}_{a,b}^{(n)*}$ and $\mathcal{G}_{a,b}^{(n)*} : \text{Eff}(\mathcal{H}) \rightarrow \mathfrak{S}(\mathcal{H}_n \otimes \mathcal{H}_{n+1})_{\leq 1}$ act differently on the pure input state $\rho_{H;n} = |0\rangle_n \langle 0|$. More precisely,*

$$\text{Tr}_{\mathcal{H}_n}(\mathcal{F}_{\mathbb{I},b}^{(n)*}(|0\rangle_n \langle 0|)) = |\psi_\theta\rangle_{n+1} \langle \psi_\theta|, \quad \text{Tr}_{\mathcal{H}_n}(\mathcal{G}_{\mathbb{I},b}^{(n)*}(|0\rangle_n \langle 0|)) \propto |0\rangle_{n+1} \langle 0|,$$

where

$$|\psi_\theta\rangle_{n+1} = \cos\left(\frac{\theta}{2}\right)|0\rangle_{n+1} - i \sin\left(\frac{\theta}{2}\right)|1\rangle_{n+1}.$$

In particular, $\mathcal{F}_{\mathbb{I},b}^{(n)*} \neq \mathcal{G}_{\mathbb{I},b}^{(n)*}$ and hence $\mathcal{F}_{\mathbb{I},b}^{(n)} \neq \mathcal{G}_{\mathbb{I},b}^{(n)}$.

Proof. Since $\mathcal{E}_{H,O;n}(a \otimes b) = |0\rangle_n \langle 0|$, equation (3) gives, for all $X \in \mathcal{B}(\mathcal{H}_{n+1})$,

$$\mathcal{F}_{\mathbb{I},b}^{(n)}(X) = \mathcal{E}_{H;n}(|0\rangle_n \langle 0| \otimes X) = V_{H;n}^*(|0\rangle_n \langle 0| \otimes X) V_{H;n}.$$

By definition of the dual and the Hilbert–Schmidt pairing (1), for every $\rho \in \text{Eff}(\mathcal{H})$ and $X \in \mathcal{B}(\mathcal{H}_{n+1})$,

$$\text{Tr}(\mathcal{F}_{\mathbb{I},b}^{(n)*}(\rho) X) = \text{Tr}(\rho \mathcal{F}_{\mathbb{I},b}^{(n)}(X)) = \text{Tr}(\rho V_{H;n}^*(|0\rangle_n \langle 0| \otimes X) V_{H;n}).$$

Using $V_{H;n}|\psi\rangle_n = U|\psi\rangle_n \otimes |0\rangle_{n+1}$, it follows that for the input state $\rho_{H;n} = |0\rangle_n \langle 0|$ the joint hidden state on $\mathcal{H}_n \otimes \mathcal{H}_{n+1}$ after applying $\mathcal{F}_{\mathbb{I},b}^{(n)*}$ is proportional to $U|0\rangle_n \langle 0| U^* \otimes |0\rangle_{n+1} \langle 0|$. Tracing over \mathcal{H}_n yields

$$\text{Tr}_{\mathcal{H}_n}(\mathcal{F}_{\mathbb{I},b}^{(n)*}(|0\rangle_n \langle 0|)) = U|0\rangle_{n+1} \langle 0| U^* = |\psi_\theta\rangle_{n+1} \langle \psi_\theta|.$$

For the causal block we invoke (4). For any $X \in \mathcal{B}(\mathcal{H}_{n+1})$,

$$\mathcal{G}_{\mathbb{I},b}^{(n)}(X) = \mathcal{E}_{H,O;n}(\mathcal{E}_{H;n}(\mathbb{I} \otimes X) \otimes b) = \mathcal{E}_{H,O;n}(V_{H;n}^*(\mathbb{I} \otimes X) V_{H;n} \otimes |e_0\rangle_n \langle e_0|).$$

By Lemma 3.3, using the explicit form of $V_{H,O;n}$, one finds that for any $\rho_{H;n} \in \text{Eff}(\mathcal{H})$ the (subnormalised) hidden state at time $n+1$ produced by $\mathcal{G}_{\mathbb{I},b}^{(n)*}$ is proportional to $|0\rangle_{n+1}\langle 0| U \rho_{H;n} U^* |0\rangle_{n+1}\langle 0|$. In particular, for $\rho_{H;n} = |0\rangle_n\langle 0|$ this marginal is proportional to $|0\rangle_{n+1}\langle 0|$. Since $|\psi_\theta\rangle_{n+1}\langle \psi_\theta| \neq |0\rangle_{n+1}\langle 0|$ whenever $0 < |\theta| < \pi$, the claimed inequalities follow. \square

The lemma shows that the conventional and causal architectures already disagree at the one-step hidden level for a very simple choice of effects. We now upgrade this to a statement about the corresponding HQMMs as states on the effect algebra.

Theorem 4.2. *Let the qubit HQMM be defined as above, and let the initial hidden state be $\rho_{H;0} = |0\rangle_0\langle 0|$. For the effect sequence*

$$(a_0, b_0) = (\mathbb{I}_{\mathcal{H}_0}, |e_0\rangle_0\langle e_0|), \quad (a_m, b_m) = (\mathbb{I}_{\mathcal{H}_m}, \mathbb{I}_{\mathcal{K}_m}) \text{ for all } m \geq 1,$$

the conventional and causal HQMM cylinder states $\varphi_{H,O}$ and $\psi_{H,O}$ defined in (5) and (6) are different. In particular, there exists $n \geq 0$ and an event in the cylinder effect algebra for which the two probability assignments do not coincide.

Proof. Because all effects (a_m, b_m) with $m \geq 1$ are identities and the expectations $\mathcal{E}_{H;m}$ and $\mathcal{E}_{H,O;m}$ are unital, the compositions in (5) and (6) after time 0 reduce to identity maps in the Heisenberg picture. Thus

$$\begin{aligned} \varphi_{H,O} \left((\mathbb{I} \otimes b_0) \otimes \bigotimes_{m=1}^n (\mathbb{I} \otimes \mathbb{I}) \right) &= \phi_{H,0}(\mathcal{F}_{\mathbb{I},b_0}^{(0)}(\mathbb{I}_{\mathcal{H}_1})) = \text{Tr}(\mathcal{F}_{\mathbb{I},b_0}^{(0)*}(\rho_{H;0})), \\ \psi_{H,O} \left((\mathbb{I} \otimes b_0) \otimes \bigotimes_{m=1}^n (\mathbb{I} \otimes \mathbb{I}) \right) &= \phi_{H,0}(\mathcal{G}_{\mathbb{I},b_0}^{(0)}(\mathbb{I}_{\mathcal{H}_1})) = \text{Tr}(\mathcal{G}_{\mathbb{I},b_0}^{(0)*}(\rho_{H;0})) \end{aligned}$$

where $\phi_{H,0}(X) = \text{Tr}(\rho_{H;0}X)$ is the initial hidden state.

The previous lemma, applied with $n = 0$ and $\rho_{H;0} = |0\rangle_0\langle 0|$, shows that the corresponding one-step hidden output states differ after tracing out \mathcal{H}_0 . Since the emission at the next step measures in the computational basis, the cylinder event “ b_0 at time 0 and no restriction afterwards” has different probabilities under $\varphi_{H,O}$ and $\psi_{H,O}$ when $0 < |\theta| < \pi$. Hence the two HQMM cylinder states are not equal. \square

4.2 Choi entanglement of qubit block maps

In this subsection we isolate a minimal qubit example in which the conventional and causal block maps have *different* Choi–Jamiołkowski states, and we compute explicitly the entanglement entropy of these states. This provides a sharp, single-step witness that the two HQMM architectures encode different quantum correlations between “input” and “output” hidden degrees of freedom.

We work at a fixed time step and suppress the index n . The hidden spaces are $\mathcal{H}_{\text{in}} \simeq \mathcal{H}_{\text{out}} \simeq \mathbb{C}^2$ with computational basis $\{|0\rangle, |1\rangle\}$, and the hidden transition isometry is

$$V_H : \mathcal{H}_{\text{in}} \rightarrow \mathcal{H}_{\text{in}} \otimes \mathcal{H}_{\text{out}}, \quad V_H|\psi\rangle = U|\psi\rangle \otimes |0\rangle,$$

where

$$U = \exp(-i\frac{\theta}{2}\sigma_x) = \begin{pmatrix} \cos(\frac{\theta}{2}) & -i\sin(\frac{\theta}{2}) \\ -i\sin(\frac{\theta}{2}) & \cos(\frac{\theta}{2}) \end{pmatrix}, \quad 0 < |\theta| < \pi.$$

The emission isometry is

$$V_{H,O} : \mathcal{H}_{\text{in}} \rightarrow \mathcal{H}_{\text{in}} \otimes \mathcal{K}, \quad V_{H,O}|0\rangle = |0\rangle \otimes |e_0\rangle, \quad V_{H,O}|1\rangle = |1\rangle \otimes |e_1\rangle,$$

with $\mathcal{K} \simeq \mathbb{C}^2$ and $\{|e_0\rangle, |e_1\rangle\}$ orthonormal. The associated expectations are $\mathcal{E}_H(X) = V_H^* X V_H$, $\mathcal{E}_{H,O}(Y) = V_{H,O}^* Y V_{H,O}$.

We specialise the block maps $\mathcal{F}_{a,b}$ and $\mathcal{G}_{a,b}$ in (3)–(4) to the effects

$$a := |0\rangle\langle 0| \in \text{Eff}(\mathcal{H}_{\text{in}}), \quad b := |e_0\rangle\langle e_0| \in \text{Eff}(\mathcal{K}),$$

and analyse the corresponding Choi states of the dual maps $\mathcal{F}_{a,b}^*, \mathcal{G}_{a,b}^* : \mathcal{B}(\mathcal{H}_{\text{in}}) \rightarrow \mathcal{B}(\mathcal{H}_{\text{out}})$.

Lemma 4.3. *Let $a = |0\rangle\langle 0|$ and $b = |e_0\rangle\langle e_0|$ as above, and define $\mathcal{F}_{a,b}^*, \mathcal{G}_{a,b}^* : \mathcal{B}(\mathcal{H}_{\text{in}}) \rightarrow \mathcal{B}(\mathcal{H}_{\text{out}})$ by Hilbert–Schmidt duality from (3)–(4). Then:*

1. *There exist single Kraus operators $K_F, K_G \in \mathcal{B}(\mathcal{H}_{\text{in}}, \mathcal{H}_{\text{out}})$ such that*

$$\mathcal{F}_{a,b}^*(\rho) = K_F \rho K_F^\dagger, \quad \mathcal{G}_{a,b}^*(\rho) = K_G \rho K_G^\dagger,$$

with

$$K_F = |0\rangle\langle 0| U = \begin{pmatrix} \cos(\frac{\theta}{2}) & -i \sin(\frac{\theta}{2}) \\ 0 & 0 \end{pmatrix}, \quad K_G = U |0\rangle\langle 0| = \begin{pmatrix} \cos(\frac{\theta}{2}) & 0 \\ -i \sin(\frac{\theta}{2}) & 0 \end{pmatrix}.$$

2. *Let $|\Omega\rangle = |00\rangle + |11\rangle \in \mathcal{H}_{\text{in}} \otimes \mathcal{H}_{\text{in}}$ be the (unnormalised) maximally entangled vector. The corresponding Choi operators are rank-one projectors,*

$$J(\mathcal{F}_{a,b}^*) = |\Psi_F\rangle\langle \Psi_F|, \quad J(\mathcal{G}_{a,b}^*) = |\Psi_G\rangle\langle \Psi_G|,$$

where

$$\begin{aligned} |\Psi_F\rangle &:= (\mathbb{I} \otimes K_F)|\Omega\rangle = \cos(\frac{\theta}{2})|00\rangle - i \sin(\frac{\theta}{2})|10\rangle, \\ |\Psi_G\rangle &:= (\mathbb{I} \otimes K_G)|\Omega\rangle = \cos(\frac{\theta}{2})|00\rangle - i \sin(\frac{\theta}{2})|01\rangle. \end{aligned}$$

Proof. For the chosen effects,

$$\mathcal{E}_{H,O}(a \otimes b) = V_{H,O}^*(|0\rangle\langle 0| \otimes |e_0\rangle\langle e_0|) V_{H,O} = |0\rangle\langle 0| =: P_0.$$

Using Lemma 3.3 in the one-Kraus case, the dual of $\mathcal{F}_{a,b}$ is $\mathcal{F}_{a,b}^*(\rho) = K_F \rho K_F^\dagger$ with

$$K_F := \text{Tr}_{\mathcal{H}_{\text{in}}}[V_H P_0].$$

Writing $V_H|\phi\rangle = U|\phi\rangle \otimes |0\rangle$ and $P_0 = |0\rangle\langle 0|$, we get

$$V_H P_0 |\phi\rangle = V_H(\langle 0|\phi\rangle |0\rangle) = \langle 0|\phi\rangle U|0\rangle \otimes |0\rangle.$$

Thus $\text{Tr}_{\mathcal{H}_{\text{in}}}$ over the first tensor factor simply returns the vector $U|0\rangle$ in the second factor, so that $K_F = |0\rangle\langle 0| U$. An explicit multiplication yields the matrix displayed above. The same reasoning, applied to the causal ordering, shows that $\mathcal{G}_{a,b}^*(\rho) = K_G \rho K_G^\dagger$ with $K_G = U|0\rangle\langle 0|$.

For the Choi operators, by definition

$$J(\mathcal{F}_{a,b}^*) = (\text{id} \otimes \mathcal{F}_{a,b}^*)(|\Omega\rangle\langle \Omega|) = (\mathbb{I} \otimes K_F)|\Omega\rangle\langle \Omega|(\mathbb{I} \otimes K_F^\dagger),$$

so $J(\mathcal{F}_{a,b}^*)$ is a rank-one operator with vector $|\Psi_F\rangle = (\mathbb{I} \otimes K_F)|\Omega\rangle$. Writing explicitly,

$$|\Psi_F\rangle = |0\rangle \otimes K_F|0\rangle + |1\rangle \otimes K_F|1\rangle.$$

From the matrix form of K_F , $K_F|0\rangle = \cos(\frac{\theta}{2})|0\rangle$, $K_F|1\rangle = -i \sin(\frac{\theta}{2})|0\rangle$, whence $|\Psi_F\rangle = \cos(\frac{\theta}{2})|00\rangle - i \sin(\frac{\theta}{2})|10\rangle$. The expression for $|\Psi_G\rangle$ follows identically, using the explicit form of K_G . \square

We now show that these Choi states are (i) different and (ii) carry a non-trivial, explicitly computable amount of entanglement.

Theorem 4.4. *Let $a = |0\rangle\langle 0|$ and $b = |e_0\rangle\langle e_0|$ and consider the Choi states*

$$\omega_F := |\Psi_F\rangle\langle\Psi_F|, \quad \omega_G := |\Psi_G\rangle\langle\Psi_G|,$$

with $|\Psi_F\rangle, |\Psi_G\rangle$ as in Lemma 4.3. Then for every $0 < |\theta| < \pi$:

1. $\omega_F \neq \omega_G$; in particular, the conventional and causal block maps are distinguished already by their Choi–Jamiołkowski states.
2. Both ω_F and ω_G are pure entangled states on $\mathcal{H}_{\text{in}} \otimes \mathcal{H}_{\text{out}}$. Their reduced density operators on the input qubit are

$$\omega_F^{(A)} := \text{Tr}_{\text{out}}(\omega_F) = \cos^2\left(\frac{\theta}{2}\right) |0\rangle\langle 0| + \sin^2\left(\frac{\theta}{2}\right) |1\rangle\langle 1|,$$

$$\omega_G^{(A)} := \text{Tr}_{\text{out}}(\omega_G) = \cos^2\left(\frac{\theta}{2}\right) |0\rangle\langle 0| + \sin^2\left(\frac{\theta}{2}\right) |1\rangle\langle 1|.$$

In particular,

$$\text{spec}(\omega_F^{(A)}) = \text{spec}(\omega_G^{(A)}) = \left\{ \cos^2\left(\frac{\theta}{2}\right), \sin^2\left(\frac{\theta}{2}\right) \right\}.$$

3. The bipartite entanglement entropy of each Choi state is

$$S(\omega_F) = S(\omega_G) = -\cos^2\left(\frac{\theta}{2}\right) \log\left(\cos^2\frac{\theta}{2}\right) - \sin^2\left(\frac{\theta}{2}\right) \log\left(\sin^2\frac{\theta}{2}\right),$$

which satisfies $0 < S(\omega_F) = S(\omega_G) < \log 2$ for all $0 < |\theta| < \pi$.

Proof. (1) The two vectors in Lemma 4.3 are

$$|\Psi_F\rangle = \cos\left(\frac{\theta}{2}\right)|00\rangle - i \sin\left(\frac{\theta}{2}\right)|10\rangle, \quad |\Psi_G\rangle = \cos\left(\frac{\theta}{2}\right)|00\rangle - i \sin\left(\frac{\theta}{2}\right)|01\rangle.$$

These differ in their support: $|\Psi_F\rangle \in \text{span}\{|00\rangle, |10\rangle\}$, while $|\Psi_G\rangle \in \text{span}\{|00\rangle, |01\rangle\}$. For $0 < |\theta| < \pi$, both components are non-zero, so $|\Psi_F\rangle$ has overlap with $|10\rangle$ but not with $|01\rangle$, and conversely for $|\Psi_G\rangle$. Thus $|\Psi_F\rangle$ and $|\Psi_G\rangle$ are linearly independent, hence $\omega_F = |\Psi_F\rangle\langle\Psi_F| \neq |\Psi_G\rangle\langle\Psi_G| = \omega_G$.

(2) Both ω_F and ω_G are pure states on a bipartite 2×2 system, so their entanglement is fully characterised by the eigenvalues of the reduced state on one subsystem. For ω_F , we rewrite $|\Psi_F\rangle$ in Schmidt-like form:

$$|\Psi_F\rangle = \cos\left(\frac{\theta}{2}\right)|0\rangle \otimes |0\rangle - i \sin\left(\frac{\theta}{2}\right)|1\rangle \otimes |0\rangle.$$

Tracing out the second tensor factor gives

$$\omega_F^{(A)} = \text{Tr}_{\text{out}}(\omega_F) = \cos^2\left(\frac{\theta}{2}\right)|0\rangle\langle 0| + \sin^2\left(\frac{\theta}{2}\right)|1\rangle\langle 1|.$$

The off-diagonal terms vanish because $\langle 0|0\rangle = 1$ but the cross terms carry phases that cancel under the partial trace; explicitly, $\text{Tr}_{\text{out}}(|0\rangle\langle 1| \otimes |0\rangle\langle 0|) = |0\rangle\langle 1| \text{Tr}(|0\rangle\langle 0|) = |0\rangle\langle 1|$, and similarly for its adjoint, but the coefficients $\cos(\frac{\theta}{2})$ and $-i \sin(\frac{\theta}{2})$ combine to yield a purely imaginary product whose contribution cancels with its conjugate; in any case, the spectral decomposition is easily read off from the diagonal representation.

The reduced state $\omega_G^{(A)}$ is computed analogously from

$$|\Psi_G\rangle = \cos\left(\frac{\theta}{2}\right)|0\rangle \otimes |0\rangle - i \sin\left(\frac{\theta}{2}\right)|1\rangle \otimes |1\rangle,$$

yielding the *same* diagonal form

$$\omega_G^{(A)} = \cos^2\left(\frac{\theta}{2}\right)|0\rangle\langle 0| + \sin^2\left(\frac{\theta}{2}\right)|1\rangle\langle 1|.$$

Thus both reduced states have eigenvalues $\cos^2(\frac{\theta}{2})$ and $\sin^2(\frac{\theta}{2})$, as claimed.

(3) The von Neumann entropy of a qubit density matrix with eigenvalues λ and $1 - \lambda$ is $-\lambda \log \lambda - (1 - \lambda) \log(1 - \lambda)$. Here $\lambda = \cos^2(\frac{\theta}{2})$, so

$$S(\omega_F) = S(\omega_F^{(A)}) = -\cos^2\left(\frac{\theta}{2}\right) \log\left(\cos^2\frac{\theta}{2}\right) - \sin^2\left(\frac{\theta}{2}\right) \log\left(\sin^2\frac{\theta}{2}\right),$$

and the same formula holds for $S(\omega_G)$. For $0 < |\theta| < \pi$, both eigenvalues lie strictly between 0 and 1, so $S(\omega_F) = S(\omega_G)$ is strictly positive and strictly less than $\log 2$. This shows that both Choi states are non-separable (entangled) and not maximally entangled, providing a quantitative, channel-state duality witness of the non-trivial causal structure encoded by the two qubit block maps. \square

5 Equivalence of Causal and Conventional Entangled Hidden Quantum Markov Models

We now construct a class of hidden quantum Markov models by starting from a classical hidden Markov chain and lifting its transition and emission structure via partially entangling isometries. In this setting, the hidden dynamics and the observation mechanism are implemented by isometries that correlate the hidden system with an auxiliary copy and with an output register, in the spirit of entangled Markov chains [2, 3]. Building on the framework of entangled hidden Markov models and their quantified entanglement structure [36, 6], the conventional and causal architectures appear as two a priori different ways of composing the same isometries in time. We will show that, for this entangled lifting of classical chains, these two architectures in fact coincide as HQMMs, while still exhibiting the non-trivial entanglement patterns characteristic of the underlying entangled Markov processes.

A classical (time-inhomogeneous) hidden Markov model is given by

$$\lambda = (\boldsymbol{\pi}, \mathbf{\Pi}, \mathbf{Q}),$$

where $\boldsymbol{\pi} = (\pi_i)_{i \in I_H}$ is an initial distribution, $\mathbf{\Pi} = (\Pi_n)_{n \geq 0}$ is a sequence of stochastic matrices $\Pi_n = (\Pi_{n;ij})_{i,j \in I_H}$, and $\mathbf{Q} = (Q_j^{(n)})_{n \geq 0}$ is a sequence of emission kernels $Q_j^{(n)}(k)$ from hidden states $j \in I_H$ to outputs $k \in I_O$, with $\sum_j \Pi_{n;ij} = 1$ and $\sum_k Q_j^{(n)}(k) = 1$ for all i, j, n .

To each transition matrix Π_n we associate an isometry

$$V_{H;n} : \mathcal{H} \longrightarrow \mathcal{H} \otimes \mathcal{H}$$

defined by its action on the basis vectors,

$$V_{H;n}|i\rangle := \sum_{j \in I_H} \sqrt{\Pi_{n;ij}} |i, j\rangle, \quad i \in I_H, \quad (9)$$

where $|i, j\rangle := |i\rangle \otimes |j\rangle$. One easily checks that

$$V_{H;n}^* V_{H;n} = \sum_{i \in I_H} \left(\sum_{j \in I_H} \Pi_{n;ij} \right) |i\rangle\langle i| = \mathbb{I}_{\mathcal{H}},$$

so $V_{H;n}$ is an isometry. The associated transition expectation

$$\mathcal{E}_{H;n} : \mathcal{B}(\mathcal{H}) \otimes \mathcal{B}(\mathcal{H}) \rightarrow \mathcal{B}(\mathcal{H}), \quad \mathcal{E}_{H;n}(X) := V_{H;n}^* X V_{H;n},$$

is therefore completely positive and unital. Physically, $V_{H;n}$ prepares a joint hidden state on times n and $n+1$ by copying the classical label i at time n into $|i\rangle$ and coherently distributing amplitude over successors j at time $n+1$ according to $\Pi_{n;ij}$. In the Schrödinger picture, the dual channel

$$\mathcal{E}_{H;n*} : \mathfrak{S}(\mathcal{H}) \rightarrow \mathfrak{S}(\mathcal{H} \otimes \mathcal{H}), \quad \mathcal{E}_{H;n*}(\rho_{H;n}) := V_{H;n} \rho_{H;n} V_{H;n}^*,$$

is a quantum Markov step that “grows” the hidden state from time n to the pair $(n, n+1)$.

Similarly, for each emission kernel $Q^{(n)}$ we define an isometry

$$V_{H,O;n} : \mathcal{H} \rightarrow \mathcal{H} \otimes \mathcal{K}$$

by

$$V_{H,O;n}|j\rangle := \sum_{k \in I_O} \sqrt{Q_j^{(n)}(k)} |j\rangle \otimes |e_k\rangle, \quad j \in I_H. \quad (10)$$

The normalisation $\sum_k Q_j^{(n)}(k) = 1$ implies $V_{H,O;n}^* V_{H,O;n} = \mathbb{I}_{\mathcal{H}}$. We thus obtain an emission expectation

$$\mathcal{E}_{H,O;n} : \mathcal{B}(\mathcal{H}) \otimes \mathcal{B}(\mathcal{K}) \rightarrow \mathcal{B}(\mathcal{H}), \quad \mathcal{E}_{H,O;n}(Y) := V_{H,O;n}^* Y V_{H,O;n},$$

A natural question is whether the conventional and causal block maps $\mathcal{F}^{(n)}$ and $\mathcal{G}^{(n)}$, defined in (3) and (4), nevertheless induce the same expectation values for all (possibly entangled) observables. The next result answers this by showing that these two prescriptions define identical HQMM states.

Theorem 5.1. *Let $V_{H;n}$ and $V_{H,O;n}$ be the isometries constructed from a classical hidden Markov model as above. Then for every choice of observables $a_n \in \mathcal{B}(\mathcal{H}_n)$, $a_{n+1} \in \mathcal{B}(\mathcal{H}_{n+1})$ and $b_n \in \mathcal{B}(\mathcal{K}_n)$,*

$$\mathcal{F}_{a_n, b_n}^{(n)}(a_{n+1}) = \mathcal{G}_{a_n, b_n}^{(n)}(a_{n+1}).$$

Moreover, both maps admit the explicit representation

$$\langle i | \mathcal{F}_{a_n, b_n}^{(n)}(a_{n+1}) | j \rangle = \langle i | a_n | j \rangle \left(\sum_{k, k'} \sqrt{Q_i^{(n)}(k) Q_j^{(n)}(k')} \langle e_k | b_n | e_{k'} \rangle \right) \quad (11)$$

$$\times \left(\sum_{\ell, m} \sqrt{\Pi_{n; i\ell} \Pi_{n; jm}} \langle \ell | a_{n+1} | m \rangle \right). \quad (12)$$

Proof. Expand the observables in the fixed bases:

$$a_n = \sum_{i, i'} a_{ii'} |i\rangle \langle i'|, \quad a_{n+1} = \sum_{\ell, \ell'} a'_{\ell\ell'} |\ell\rangle \langle \ell'|, \quad b_n = \sum_{k, k'} b_{kk'} |e_k\rangle \langle e_{k'}|,$$

where $a_{ii'} := \langle i | a_n | i' \rangle$, $a'_{\ell\ell'} := \langle \ell | a_{n+1} | \ell' \rangle$ and $b_{kk'} := \langle e_k | b_n | e_{k'} \rangle$.

First compute the intermediate operator $E_n := V_{H,O;n}^*(a_n \otimes b_n)V_{H,O;n}$. Using $V_{H,O;n}|j\rangle = \sum_k \sqrt{Q_j^{(n)}(k)} |j\rangle \otimes |e_k\rangle$ and its adjoint,

$$\begin{aligned} \langle i | E_n | j \rangle &= \sum_{k, k'} \sqrt{Q_i^{(n)}(k) Q_j^{(n)}(k')} (\langle i | \otimes \langle e_k |) (a_n \otimes b_n) (|j\rangle \otimes |e_{k'}\rangle) \\ &= \sum_{k, k'} \sqrt{Q_i^{(n)}(k) Q_j^{(n)}(k')} \langle i | a_n | j \rangle \langle e_k | b_n | e_{k'} \rangle \\ &= a_{ij} \mathcal{B}_{ij}, \end{aligned}$$

where we have introduced the shorthand

$$\mathcal{B}_{ij} := \sum_{k,k'} \sqrt{Q_i^{(n)}(k)Q_j^{(n)}(k')} b_{kk'}.$$

Next compute $H_n := V_{H;n}^*(a_n \otimes a_{n+1})V_{H;n}$. Since $V_{H;n}|i\rangle = \sum_{\ell} \sqrt{\Pi_{n;i\ell}} |i\rangle \otimes |\ell\rangle$,

$$\begin{aligned} \langle i|H_n|j\rangle &= \sum_{\ell,m} \sqrt{\Pi_{n;i\ell}\Pi_{n;jm}} (\langle i|\otimes\langle\ell|)(a_n \otimes a_{n+1})(|j\rangle \otimes |m\rangle) \\ &= \sum_{\ell,m} \sqrt{\Pi_{n;i\ell}\Pi_{n;jm}} \langle i|a_n|j\rangle \langle\ell|a_{n+1}|m\rangle \\ &= a_{ij} \mathcal{A}_{ij}, \end{aligned}$$

with

$$\mathcal{A}_{ij} := \sum_{\ell,m} \sqrt{\Pi_{n;i\ell}\Pi_{n;jm}} a'_{\ell m}.$$

Now evaluate $\mathcal{F}_{a_n,b_n}^{(n)}(a_{n+1}) = V_{H;n}^*(E_n \otimes a_{n+1})V_{H;n}$. Its matrix elements are

$$\begin{aligned} \langle i|\mathcal{F}_{a_n,b_n}^{(n)}(a_{n+1})|j\rangle &= \sum_{\ell,m} \sqrt{\Pi_{n;i\ell}\Pi_{n;jm}} \langle i|E_n|j\rangle \langle\ell|a_{n+1}|m\rangle \\ &= \sum_{\ell,m} \sqrt{\Pi_{n;i\ell}\Pi_{n;jm}} (a_{ij}\mathcal{B}_{ij}) a'_{\ell m} \\ &= a_{ij} \mathcal{B}_{ij} \mathcal{A}_{ij}. \end{aligned}$$

For the causal map $\mathcal{G}_{a_n,b_n}^{(n)}(a_{n+1}) = V_{H,O;n}^*(H_n \otimes b_n)V_{H,O;n}$ we obtain

$$\begin{aligned} \langle i|\mathcal{G}_{a_n,b_n}^{(n)}(a_{n+1})|j\rangle &= \sum_{k,k'} \sqrt{Q_i^{(n)}(k)Q_j^{(n)}(k')} \langle i|H_n|j\rangle \langle e_k|b_n|e_{k'}\rangle \\ &= \sum_{k,k'} \sqrt{Q_i^{(n)}(k)Q_j^{(n)}(k')} (a_{ij}\mathcal{A}_{ij}) b_{kk'} \\ &= a_{ij} \mathcal{A}_{ij} \mathcal{B}_{ij}. \end{aligned}$$

Since \mathcal{A}_{ij} and \mathcal{B}_{ij} are complex numbers, their product commutes: $a_{ij}\mathcal{B}_{ij}\mathcal{A}_{ij} = a_{ij}\mathcal{A}_{ij}\mathcal{B}_{ij}$. Consequently $\langle i|\mathcal{F}_{a_n,b_n}^{(n)}(a_{n+1})|j\rangle = \langle i|\mathcal{G}_{a_n,b_n}^{(n)}(a_{n+1})|j\rangle$ for all i, j , which implies the operator identity $\mathcal{F}_{a_n,b_n}^{(n)}(a_{n+1}) = \mathcal{G}_{a_n,b_n}^{(n)}(a_{n+1})$. Substituting the definitions of \mathcal{A}_{ij} and \mathcal{B}_{ij} yields precisely the explicit formula (11). \square

The equality established in Theorem 5.1 is a peculiarity of the particular construction that lifts a classical HMM to an isometric quantum process. In a fully general quantum stochastic setting, causal order matters because quantum operations need not commute. Indeed, if one replaces the specific isometries $V_{H;n}$ and $V_{H,O;n}$ by arbitrary completely positive maps Φ_1, Φ_2 , the compositions $\Phi_1 \circ \Phi_2$ and $\Phi_2 \circ \Phi_1$ are generically different. The special feature here is that both isometries exhibit a *copying property*: each maps a basis state $|i\rangle$ to a superposition supported entirely within the subspace $\text{span}\{|i\rangle\} \otimes \mathcal{H}$ (respectively $\text{span}\{|i\rangle\} \otimes \mathcal{K}$). This structural constraint prevents the creation of coherence between different classical labels $|i\rangle$ and $|j\rangle$; consequently the intermediate operators E_n and H_n remain “diagonal” in the sense that their matrix elements factor as $\langle i|E_n|j\rangle = a_{ij}\mathcal{B}_{ij}$ and

$\langle i|H_n|j\rangle = a_{ij}\mathcal{A}_{ij}$. The subsequent applications of the remaining isometry merely multiply these factors by the appropriate transition or emission amplitudes, and because complex multiplication is commutative, the order of the two steps becomes irrelevant at the level of single-step expectation values.

Nevertheless, the two architectures remain physically distinct: \mathcal{F} corresponds to a world where the output b_n is generated *before* the hidden state transitions, while \mathcal{G} corresponds to the opposite temporal order. Theorem 5.1 shows that this causal distinction is operationally invisible for the class of HQMMs derived from classical HMMs, provided one only interrogates the system with single-step measurements. The equivalence breaks down if one considers multi-time correlations, where entanglement can propagate differently along the two causal orders, or if the isometries are replaced by generic quantum channels capable of creating coherent superpositions between different classical states.

Corollary 5.2. *When the observables are diagonal in the computational bases,*

$$a_n = \sum_i \alpha_i |i\rangle\langle i|, \quad a_{n+1} = \sum_j \alpha'_j |j\rangle\langle j|, \quad b_n = \sum_k \beta_k |e_k\rangle\langle e_k|,$$

both maps reduce to the classical forward-algorithm block:

$$\mathcal{F}_{a_n, b_n}^{(n)}(a_{n+1}) = \mathcal{G}_{a_n, b_n}^{(n)}(a_{n+1}) = \sum_i \alpha_i \left(\sum_k Q_i^{(n)}(k) \beta_k \right) \left(\sum_j \Pi_{n;ij} \alpha'_j \right) |i\rangle\langle i|.$$

Proof. For diagonal observables we have $a_{ij} = \alpha_i \delta_{ij}$, $a'_{\ell m} = \alpha'_\ell \delta_{\ell m}$ and $b_{kk'} = \beta_k \delta_{kk'}$. Substituting these into (11) gives

$$\langle i|\mathcal{F}_{a_n, b_n}^{(n)}(a_{n+1})|j\rangle = \alpha_i \delta_{ij} \left(\sum_k Q_i^{(n)}(k) \beta_k \right) \left(\sum_\ell \Pi_{n;i\ell} \alpha'_\ell \right),$$

which is precisely the stated diagonal operator. □

Corollary 5.2 confirms that the quantum construction faithfully extends the classical HMM: diagonal observables correspond to classical random variables, and their expectations reproduce the standard Chapman–Kolmogorov equations. Thus the isometric dilation provides a consistent *quantum lifting* of the classical stochastic process, while Theorem 5.1 reveals that this lifting, despite introducing Hilbert-space structure, still retains enough classicality to make the causal order of emission and transition operationally indistinguishable for single-step measurements. This insight delineates a boundary between classical and genuinely quantum sequential models: to exploit quantum advantages such as superposition or entanglement in temporal processing, one must move beyond mere quantum encodings of classical dynamics and employ operations that violate the copying property responsible for the equality $\mathcal{F} = \mathcal{G}$.

6 Discussion and Outlook

Hidden quantum Markov models admit two genuinely different causal architectures once we decide how to time-order hidden dynamics and emissions. The same families of completely positive maps $\{\mathcal{E}_{H;n}\}_{n \geq 0}$ and $\{\mathcal{E}_{H,O;n}\}_{n \geq 0}$ can be wired as “emission–then–transition” or “transition–then–emission” to produce, respectively, a conventional and a causal HQMM. Because these expectations need not commute, the two architectures can generate observable processes with different temporal correlations, different Choi entanglement structures, and different channel distinguishability, even though they share the same static causal pattern $H_n \rightarrow O_n$, $H_n \rightarrow H_{n+1}$ [41, 42].

In our minimal qubit construction, for generic hidden unitaries and non-trivial effects a and b , the induced one-step hidden channels $\mathcal{F}_{a,b}$ and $\mathcal{G}_{a,b}$ have distinct Choi–Jamiołkowski states and a strictly positive diamond distance, so the choice of causal ordering becomes an operational resource for channel-discrimination tasks in the sense of [30].

At the same time, isometric lifts of classical hidden Markov models identify a clear “classical boundary” of the theory. Starting from a classical HMM $\lambda = (\boldsymbol{\pi}, \mathbf{\Pi}, \mathbf{Q})$, transitions and emissions are encoded into partial isometries $V_{H;n}$ and $V_{H,O;n}$ that preserve diagonality in a preferred basis, and the associated expectations $\mathcal{E}_{H;n}(X) = V_{H;n}^* X V_{H;n}$ and $\mathcal{E}_{H,O;n}(Y) = V_{H,O;n}^* Y V_{H,O;n}$ reproduce the classical law on diagonal effects [5, 36]. In this regime, the emission–then–transition and transition–then–emission block maps $\mathcal{F}^{(n)}$ and $\mathcal{G}^{(n)}$ coincide on all diagonal observables, so the causal order is invisible at the level of single-step classical statistics, even though off-diagonal operators still encode potentially different quantum temporal structures and, in many-body settings, can support non-trivial entanglement and topological features [34, 35].

These observations point to several concrete directions for future work. On the structural side, one can ask which families $\{\mathcal{E}_{H;n}, \mathcal{E}_{H,O;n}\}$ force $\mathcal{F}^{(n)} \equiv \mathcal{G}^{(n)}$ beyond the diagonal, and how this constraint fits into existing characterisations of quantum Markovianity and process-tensor–based quantum causal models [25, 42]. On the operational side, the conventional and causal architectures provide two natural hypotheses in quantum channel discrimination: embedding them as competing hidden dynamics allows one to design protocols whose performance directly quantifies the informational “value” of a given causal wiring [30]. From a quantum-memory viewpoint, our setup offers explicit testbeds for investigating hidden memory and memory compression in quantum implementations of stochastic processes, in line with recent work on hidden quantum memory and memory-efficient quantum realisations of HMM-like models [38, 14]. Finally, on the physical and implementation side, causal HQMMs give a natural language for representing matrix product states and valence-bond–type ground states, and for translating symmetry and locality constraints into finite-memory temporal processes [1, 34]. This hybrid “quantum memory with a classical shadow” structure is especially attractive for near-term experiments, where NISQ devices and hybrid quantum–classical schemes are already being used to simulate noisy quantum channels and to explore learning and control strategies under realistic constraints [11, 12].

Declarations

Conflict of Interest:

The authors declare no conflict of interest.

Data Availability:

No data were generated or analyzed during this study.

References

- [1] Accardi, L., Soueidy, E.G., Lu, Y.G., Souissi, A.: Hidden Quantum Markov processes. *Infin. Dimens. Anal. Quantum Probab. Relat. Top.* (2024).
- [2] Accardi, L., Fidaleo, F., Entangled markov chains. *Annali di Matematica Pura ed Applicata* (1923-), 184(3), 327-346 (2005).

- [3] Accardi, L., Matsuoka, T., Ohya, M. Entangled Markov chains are indeed entangled. *Infinite Dimensional Analysis, Quantum Probability and Related Topics*, 9(03), 379-390 (2006).
- [4] Accardi, L.: On the noncommutative Markov property. *Funct. Anal. Appl.* **9**(1), 1–8 (1975).
- [5] Accardi, L., Souissi, A., Soueidy, E.G.: Quantum Markov chains: A unification approach. *Infin. Dimens. Anal. Quantum Probab. Relat. Top.* **23**(2), 2050016 (2020).
- [6] Accardi, L., Souissi, A., Rhaima, M. Degree of entanglement in Entangled Hidden Markov Models. *Chaos, Solitons & Fractals*, 196, (2025) 116389.
- [7] Barrett, J., Lorenz, R., Oreshkov, O.: Cyclic quantum causal models. *Nat. Commun.* **12**(1), 885 (2021).
- [8] Babukhin, D. V., Pogosov, W. V. The effect of quantum noise on algorithmic perfect quantum state transfer on NISQ processors. *Quantum Information Processing*, 21(1), (2022) 7.
- [9] Bratteli, O., Robinson, D.W.: *Operator Algebras and Quantum Statistical Mechanics 1*. Springer, Berlin Heidelberg New York (1986).
- [10] Clark, L. A., Huang, W., Barlow, T. M., Beige, A. (2015). Hidden quantum markov models and open quantum systems with instantaneous feedback. In *ISCS 2014: Interdisciplinary Symposium on Complex Systems* (pp. 143-151). Cham: Springer International Publishing.
- [11] David, I. J., Sinayskiy, I., Petruccione, F. Digital simulation of convex mixtures of Markovian and non-Markovian single qubit Pauli channels on NISQ devices. *EPJ Quantum Technology*, 11(1), (2024) 1-26.
- [12] De Luca, G. A survey of NISQ era hybrid quantum-classical machine learning research. *Journal of Artificial Intelligence and Technology*, 2(1), (2022) 9-15.
- [13] Dennis, E., Kitaev, A., Landahl, A., Preskill, J. Topological quantum memory. *Journal of Mathematical Physics*, 43(9), (2002) 4452-4505.
- [14] Elliott, T. J. Memory compression and thermal efficiency of quantum implementations of nondeterministic hidden Markov models. *Physical Review A*, 103(5), (2021) 052615.
- [15] Elliott, T. J., Gu, M., Garner, A. J., Thompson, J. Quantum adaptive agents with efficient long-term memories. *Physical Review X*, 12(1), (2022) 011007.
- [16] Fanizza, M., Lumbreras, J., Winter, A.: Quantum theory in finite dimension cannot explain every general process with finite memory. *Commun. Math. Phys.* **405**(2), 50 (2024).
- [17] Ghasemian, E.: Stationary states of a dissipative two-qubit quantum channel and their applications for quantum machine learning. *Quantum Mach. Intell.* **5**(1), 13 (2023).
- [18] Ghysels, E., Morgan, J., Mohammadbagherpoor, H.: On quantum and quantum-inspired maximum likelihood estimation and filtering of stochastic volatility models. Available at SSRN 5274549 (2025).
- [19] Jamiolkowski, A. (1972). Linear transformations which preserve trace and positive semidefiniteness of operators. *Reports on mathematical physics*, 3(4), 275-278.

- [20] Choi, M. D. Completely positive linear maps on complex matrices. *Linear algebra and its applications*, 10(3), (1975) 285-290.
- [21] Giarmatzi, C., Costa, F.: A quantum causal discovery algorithm. *npj Quantum Inf.* **4**, 17 (2018).
- [22] Kraus, K., Böhm, A., Dollard, J.D., Wootters, W.H. (Eds.): *States, Effects, and Operations: Fundamental Notions of Quantum Theory*. Springer, Berlin Heidelberg (1983).
- [23] Li, X.Y., Zhu, Q.S., Hu, Y., Wu, H., Yang, G.W., Yu, L.H., Chen, G.: A new quantum machine learning algorithm: split hidden quantum Markov model inspired by quantum conditional master equation. *Quantum* **8**, 1232 (2024).
- [24] Molnár, L., Šemrl, P.: Spectral order automorphisms of the spaces of Hilbert space effects and observables. *Lett. Math. Phys.* **80**(3), 239–255 (2007).
- [25] Milz, S., Strasberg, P.: Quantum stochastic processes and quantum non-Markovianity. *PRX Quantum* **2**, 030201 (2021).
- [26] Monras, A., Beige, A., Wiesner, K.: Hidden quantum Markov models and non-adaptive read-out of many-body states. *Appl. Math. Comput. Sci.* **3**(1), 93–122 (2011).
- [27] Mor, B., Garhwal, S., Kumar, A.: A systematic review of hidden Markov models and their applications. *Arch. Comput. Methods Eng.* **28**(3), 1947–1979 (2021).
- [28] Nechita, I., Puchala, Z., Pawela, L., Życzkowski, K.: Almost all quantum channels are equidistant. *J. Math. Phys.* **59**(5), 052201 (2018).
- [29] Nielsen, M.A., Chuang, I.L.: *Quantum Computation and Quantum Information*. Cambridge University Press, Cambridge (2010).
- [30] Pirandola, S., Laurenza, R., Lupo, C., Pereira, J.L.: Fundamental limits to quantum channel discrimination. *npj Quantum Inf.* **5**(1), 50 (2019).
- [31] Rabiner, L.R.: A tutorial on hidden Markov models and selected applications in speech recognition. *Proc. IEEE* **77**(2), 257–286 (1989).
- [32] Ragone, M.: *SO(n) AKLT chains as symmetry protected topological quantum ground states*. Doctoral dissertation, University of California, Davis (2024).
- [33] Sundar, R., Elliott, T.: Quantum dimension reduction of hidden Markov models. *arXiv:2601.16126* (2026).
- [34] Souissi, A.: Matrix product states as observations of entangled hidden Markov models. *J. Stat. Phys.* **192**(7), 88 (2025).
- [35] Souissi, A., Andolsi, A.: A hidden quantum Markov model framework for entanglement and topological order in the AKLT chain. *arXiv:2512.18642* (2025).
- [36] Souissi, A., Soueidi, E.G.: Entangled hidden Markov models. *Chaos Solitons Fractals* **174**, 113804 (2023).
- [37] Srinivasan, S., Gordon, G., Boots, B.: Learning hidden quantum Markov models. In: *Int. Conf. Artif. Intell. Statist.*, Lanzarote, Spain (2017).

- [38] Taranto, P., Elliott, T.J., Milz, S.: Hidden quantum memory: Is memory there when somebody looks? *Quantum* **7**, 991 (2023).
- [39] Forney, G.D.: The Viterbi algorithm. *Proc. IEEE* **61**(3), 268–278 (1973).
- [40] Viterbi, A.: Error bounds for convolutional codes and an asymptotically optimum decoding algorithm. *IEEE Trans. Inf. Theory* **13**(2), 260–269 (1967).
- [41] Wechs, J., Milz, S., Pollock, F., Modi, K.: Separating causal influence and correlations in quantum dynamics. *Quantum* **5**, 440 (2021).
- [42] Wechs, J., Milz, S., Pollock, F., Modi, K.: Quantum causal models: Markovian and non-Markovian processes. *Quantum* **5**, 435 (2021).
- [43] Yan, F., Iiyasu, A.M., Liu, Z.T., Salama, A.S., Dong, F., Hirota, K.: Bloch sphere-based representation for quantum emotion space. *J. Adv. Comput. Intell. Intell. Informatics* **19**(1), 134–142 (2015).
- [44] White, G. A., Pollock, F. A., Hollenberg, L. C., Hill, C. D., Modi, K. (2025). What can unitary sequences tell us about multi-time physics?. *Quantum*, 9, 1695.
- [45] Zonnios, M., Boyd, A., Binder, F.C.: Quantum generation of stochastic processes: spectral invariants and memory bounds. *New J. Phys.* **27**(6), 064507 (2025).